J Mol Model (2012) 18:2501–2512
DOI 10.1007/s00894-011-1268-0

ORIGINAL PAPER

Metastable region of phase diagram: optimum parameter range for processing ultrahigh molecular weight polyethylene blends

Jing-Gang Gai · Yuan Zuo

Received: 12 April 2011 / Accepted: 3 October 2011 / Published online: 27 October 2011

Abstract Numerous studies suggest that two-phase morphology and thick interface are separately beneficial to the viscosity reduction and mechanical property maintainence of the matrix when normal molecular weight polymer (NMWP) is used for modification of ultrahigh molecular weight polyethylene (UHMWPE). Nevertheless, it is very difficult to obtain a UHMWPE/NMWP blend which may demonstrate both two-phase morphology and thick interface. In this work, dissipative particle dynamics simulations and Flory-Huggins theory are applied in predicting the optimum NMWP and the corresponding conditions, wherein the melt flowability of UHMWPE can be improved while its mechanical properties can also be retained. As is indicated by dissipative particle dynamics simulations and phase diagram calculated from Flory-Huggins theory, too small Flory-Huggins interaction parameter (χ) and molecular chain length of NMWP (N_{NMWP}) may lead to the formation of a homogeneous phase, whereas very large interfacial tension and thin interfaces might also appear when parameters N_{NMWP} and χ are too large. When these parameters are located in the metastable region of the phase diagram, however, two-phase morphology occurs and interfaces of the blends are extremely thick. Therefore, metastable state is found to be advisable for both the viscosity reduction and mechanical property improvement of the UHMWPE/NMWP blends.

Keywords DPD · Metastable region · Phase diagram · UHMWPE

J.-G. Gai (✉) · Y. Zuo
State Key Laboratory of Polymer Materials Engineering,
Polymer Research Institute of Sichuan University,
Chengdu, Sichuan 610065, China
e-mail: gaijinggang@scu.edu.cn

Introduction

In recent decades, ultrahigh molecular weight polyethylene (UHMWPE) has attracted considerable attention for its outstanding properties, especially its excellent friction and wear characteristics, high notched impact strength, energy absorption capacity at high loading rates and extremely low embittlement temperatures. It can be used in a number of specific areas including ballistics composite materials, bearing components and medical materials in total joint replacement [1–3]. However, it has also baffled researchers of academia and industry alike for several difficulties existed in its processing, notably, its melt viscosity is extremely high (10^8 Pa·s) and it can hardly flow above its melting point because of its high molecular weight. As a result, conventional thermoplastic processing techniques cannot be used for its processing except for compression molding or ram extrusion. Numerous efforts have been devoted to solve this processing issue [4–10].

An effective route is to reduce the melt viscosity by mixing UHMWPE with normal molecular weight polymer (NMWP) such as high density polyethylene (HDPE) [11], low density polyethylene (LDPE) [12], polypropylene (PP) [13], polyethylene glycol (PEG) [14], and polylactic acid (PLA) [15]. According to Takeshi S, Liu GD and others, some NMWP like LDPE and PP can conveniently and effectively reduce the viscosity of UHMWPE as well as retain or even enhance its mechanical properties [15–18]. Unfortunately, most other NMWP may cause a marked decrease in some of its desirable properties such as izod notched impact strength [19]. Even for LDPE and PP, the favorable mechanical properties can only be maintained under certain conditions. Therefore, it is of great significance to perform an exhaustive search for the types of NMWP and determine their corresponding conditions so

that the melt flowability of UHMWPE can be improved while its mechanical properties can also be retained.

To find out the optimum NMWP and the corresponding conditions, factors which may influence the melt flowabilities and mechanical properties of UHMWPE/NMWP blends need to be determined first. Previous studies showed that melt flowabilities and mechanical properties depend critically on their phase morphologies and interfacial properties [20–23]. In the cases of the UHMWPE/LDPE blend and UHMWPE/LLDPE blend, when they were heated to above the melting points of conventional polyethylene LDPE and LLDPE, the internal entanglement structures of UHMWPE powders were not destroyed although conventional polyethylene behaved more like a liquid [24]. UHMWPE powders suspended in the liquid phase of the LDPE or LLDPE, and the blends displayed two-phase morphologies in mesoscale. Resultantly, the mixture was processable by conventional injection molding machines and screw extruders. Due to the thick interfaces of the UHMWPE/NMWP blends, there was no substantial decrease of its excellent mechanical properties such as tensile strength and impact strength [15]. Similarly, in the UHMWPE/PP blend, the molten PP preferred to flow into the gaps between UHMWPE particles instead of wholly penetrating into the UHMWPE particles [16, 17]. Consequently, the addition of PP significantly improved the melt flowability of UHMWPE and the die pressure was very stable during extrusion. Besides, the addition of PP (10 wt %) to UHMWPE can improve both the strength at break and the izod notched impact strength to some extent [25]. Therefore, two-phase morphologies and thick interface are respectively beneficial to the viscosity reductions and mechanical property maintenance of the UHMWPE/NMWP blends.

Some unfavorable properties, nevertheless, also existed in the UHMWPE/NMWP blends when homogeneous phase morphologies occur. In the UHMWPE/HDPE blend, for instance, HDPE rich phase could not be distinguished and a homogeneous phase appeared in the crystal morphologies of the blend [16]. The molten HDPE rapidly penetrated into the UHMWPE domains during processing because of the good miscibility of the two polymers. With increasing plasticating time, no sufficient HDPE melt existed in the gaps between the particles, which hinders the plasticating of the UHMWPE/HDPE blends. Consequently, the extrusion of the UHMWPE/HDPE blend with a general single-screw extruder was exceedingly difficult. What's worse, the die pressure was very high and blockades occurred from time to time. Therefore, homogeneous phase structures are unfavorable to the flowability improvement of the matrix when NMWP is used to modify UHMWPE.

As is indicated by the above mentioned investigations, two-phase morphologies and thick interface are respectively beneficial to the viscosity reductions and the mechanical property maintenance of the UHMWPE/NMWP blends. The parameters of molecular chain length (N), Flory-Huggins interaction parameter (χ) and volume fraction of each component (ϕ) are in turn the main factors affecting the phase morphologies and interfacial properties of polymer blends. Therefore, once the optimal parameter range in which two-phase morphologies and thick interface simultaneously occur is defined, the processing conditions under which high melt flowability and mechanical property can be obtained will also be determined. Presently, the optimization of these parameters mainly depends on experimental means, but it is very difficult to undertake an exhaustive study on the phase morphologies and interfacial properties of all of the UHMWPE/NMWP blends on various conditions. Hence, it is significant to find a method by which one can predict the optimum parameter range, wherein the melt flowability of UHMWPE can be improved while its mechanical properties can also be retained. Dissipative particle dynamics (DPD) simulation and Flory-Huggins theoretical calculation have been found capable to provide valuable mesoscopic insights into the phase morphologies and interfacial properties of the immiscible polymer systems, such as the interfacial thickness (D) and the interfacial tension.

Some studies indicated that soft sphere DPD method can be used to investigate the phase morphologies and interfacial behaviors of realistic polymer blends [26, 27] although dynamics in the melts is qualitatively different between the DPD model and a more realistic system. As an example of such application, Groot and Warren tested the DPD model on simulating the interfacial tension between incompatible components and derived a master curve for that in terms of the Flory–Huggins interaction parameter. By comparing the curve with the experimental data on polystyrene/polymethyl methacrylate (PS/PMMA) interfacial tension [28], they found that DPD calculated results can be used to quantitatively predict some properties of the real systems [29–31]. Groot et al. reported that one may obtain the parameters in DPD directly from experimental interaction parameters by systematical coarse graining, [32]. Besides, Wijmans et al. have constructed a master equation by which one can make a quantitative comparison between the simulations and the experimental data [33].

In the present work, the DPD method is employed to study phase morphologies, interfacial tensions and interfacial thickness of binary UHMWPE/NMWP blends. Phase diagram calculated from Flory-Huggins theory is also adopted here to investigate the effects of parameters χ and N on interfacial properties and phase morphologies. Based on the DPD simulated results and phase diagram, we have predicted the optimum ranges of parameters χ and N, in which the UHMWPE/NMWP blends demonstrate both two-phase morphologies and thick interfaces.

Theoretical background

Phase diagram

The Flory-Huggins (F-H) expression for the free energy density of mixing of component 1 with component 2 is given by [34–37]

$$\frac{F_{mix}}{k_B T} = \frac{\phi_1 \ln \phi_1}{N_1} + \frac{\phi_2 \ln \phi_2}{N_2} + \chi \phi_1 \phi_2, \quad (1)$$

where k_B and T are Boltzmann constant and the absolute temperature. The first two terms on the right of Eq. 1 represent the combinatorial entropies for random mixtures of chain molecules, while the last term provides pairwise interactions between randomly mixed chain units.

A phase diagram, including regions of stability, instability, and metastability, can be constructed to summarize the phase behavior of the mixture. The binodal curve is determined by the common tangent of the free energy at the compositions ϕ^{I} and ϕ^{II} corresponding to the two equilibrium phases

$$\left(\frac{\partial F_{mix}}{\partial \phi}\right)_{\phi=\phi^I} = \left(\frac{\partial F_{mix}}{\partial \phi}\right)_{\phi=\phi^{II}} \quad (2)$$

i.e., the curve is calculated by simultaneously solving the following two equations

$$\ln\left(\frac{\phi_1^I}{\phi_1^{II}}\right) + (\phi_1^{II} - \phi_1^I)(1 - N_1/N_2) + \chi N_1[(1-\phi_1^I)^2 - (1-\phi_1^{II})^2] = 0 \quad (3)$$

$$\ln\left(\frac{1-\phi_1^I}{1-\phi_1^{II}}\right) + (\phi_1^I - \phi_1^{II})(1 - N_2/N_1) + \chi N_2[(\phi_1^I)^2 - (\phi_1^{II})^2] = 0 \quad (4)$$

where ϕ_1^I and ϕ_1^{II} are the volume fractions of polymer 1 in the two coexisting phases labeled I and II.

The spinodal curve defines the boundary between unstable and metastable mixtures. Thermodynamically, the spinodal condition is defined by

$$\partial^2 F_{mix}/\partial {\phi_1}^2 = 0 \quad (5)$$

DPD simulation

In the DPD simulation, the time evolution of motion for a set of interacting particles is governed by Newton's equation [38]

$$\frac{dr_i}{dt} = v_i; \quad \frac{dv_i}{dt} = f_i \quad (6)$$

where $\mathbf{r}_i$ and $\mathbf{v}_i$ are the position and the velocity of the ith particle. In this method, the force acting on a particle i ($\mathbf{f}_i$) contains conservative force $\mathbf{F}^{\mathrm{C}}$, dissipative force $\mathbf{F}^{\mathrm{D}}$, and random force $\mathbf{F}^{\mathrm{R}}$

$$f_i = \sum_{j \neq i} (F_{ij}^C + F_{ij}^D + F_{ij}^R). \quad (7)$$

The sum runs over all other particles within a certain cutoff radius r_c. For simplicity, r_c is always used as the unit of length, r_c=1. The three parts of $\mathbf{f}_i$ are given by

$$F_{ij}^C = \begin{cases} a_{ij}(1 - r_{ij})e_{ij} & (r_{ij} < r_c) \\ 0 & (r_{ij} \geq r_c). \end{cases} \quad (8)$$

$$F_{ij}^D = -\kappa \omega^D(r_{ij})(e_{ij} \cdot v_{ij})e_{ij} \quad (9)$$

$$F_{ij}^R = \sigma \omega^R(r_{ij}) \zeta_{ij} \Delta t^{-1/2} e_{ij}, \quad (10)$$

where $\mathbf{r}_{ij} = \mathbf{r}_i - \mathbf{r}_j$, $r_{ij} = -\mathbf{r}_{ij}|$, $\mathbf{e}_{ij} = \mathbf{r}_{ij}/r_{ij}$, and $\mathbf{v}_{ij} = \mathbf{v}_i - \mathbf{v}_j$. ζ_{ij} is a random number with zero mean and unit variance. a_{ij} is a maximum repulsion between particles i and j. ω^{D} and ω^{R} are weighting functions, and they vanish for $r > r_c$. NVT ensemble was used for DPD simulations. F^{D} and F^{R} act as heat sink and source, respectively, so their combined effect is a thermostat. Español and Warren have shown that there is the following fluctuation-dissipation theorem in the dissipative force and the random force [39]

$$\omega^D(r) = [\omega^R(r)]^2, \ \sigma^2 = 2\kappa k_B T. \quad (11)$$

The weight functions are chosen simply by

$$\omega^D(r) = [\omega^R(r)]^2 = \begin{cases} (1-r)^2 & (r < r_c) \\ 0 & (r \geq r_c). \end{cases} \quad (12)$$

The parameters characterizing the repulsion between the particles in DPD are directly related to the parameter χ [38, 40]. If the system has i and j components or beads interacting with each other and if one chooses a_{ii}=a_{jj} and assumes that ρ_i+ρ_j is approximately constant, then, according to Groot and Warren [38], the mapping relation is

$$\chi = \frac{2\alpha(a_{ij} - a_{ii})(\rho_i + \rho_j)}{k_B T}, \quad (13)$$

where α is a parameter related to the pair-correlation function $g(r)$, which is expressed as a function of the reduced coordinate r=$\mathbf{r}/r_c$, and ρ_i+ρ_j=ρ is the density of the system. The conservative interaction strength α_{ij} is chosen according to the linear relation with Flory–Huggins χ parameters for polymers [38]

$$\alpha_{ij} = \alpha_{ii} + 3.27\chi_{ij} \quad (\rho = 3). \quad (14)$$

The interaction parameter between the same type beads α_{ii} equals 25. In the present study, we estimate χ of component pairs from the solubility parameters using Eq. 15 [40]

$$\chi = \frac{V_{bead}(\delta_i - \delta_j)^2}{RT}, \quad (15)$$

where V_{bead} is the average molar volume of the beads, and δ_i and δ_j are the solubility parameters of beads i and j, respectively [41]. The solubility parameters can be obtained by using quantitative structure property relationship methods [42]. Equation 15 shows that varying interaction parameter can embody the effect of temperature (T) change on the system. So, the effect of temperature can be studied indirectly by analyzing the influence of interaction parameter on the system in this work. For detail comments on them, refer to Groot and Warren's work [38].

In this work, we perform DPD simulations on the UHMWPE/NMWP blends in a cell of size $32\times32\times32$, with the bead density ρ=3. For convenience, the particle mass m and k_BT were all taken as units. The time step Δt, harmonic spring constant and friction coefficient κ were taken as 0.05, 4.0 and 4.5, respectively [29, 43–46]. The total simulation times of 2×10^5 DPD steps were carried out for a DPD simulation in this work. The blend UHMWPE/NMWP employed in the DPD simulations is based on volume relation.

The number of beads in each molecule is determined by the degree of polymerization and the characteristic ratio (C_n) of the polymer. The expression for the DPD chain length (N_{DPD}) is [47]

$$N_{DPD} = \frac{M_p}{M_m C_n}, \quad (16)$$

where M_p is the polymer molar weight, M_m is the monomer molar weight and C_n is the characteristic ratio. As for UHMWPE, the characteristic ratio, monomer molar weight, average molar volume of the bead, surface tension (σ), solubility parameter, molecular weight and the corresponding DPD chain lengths are listed in Table 1.

In the present work, in order to investigate the phase morphologies and the interfacial properties of the UHMWPE/NMWP blends, we have used the periodic boundary conditions and the largest possible system within the calculating capacity of our computers. However, the realistic UHMWPE particle is so large in size that it is still beyond our simulated system. Therefore, the formation of particles can not be observed in the DPD simulations. For polymer blends, their phase morphologies and interfacial properties, such as the interfacial thickness and the interfacial tension can be simulated by DPD, but it is still hardly possible to determine which polymer blend falls in the metastable zone by the DPD simulation without using F-H theory.

Results and discussion

The investigations mentioned in the introduction indicate that two-phase morphology and thick interface are respectively beneficial to the viscosity reduction and mechanical properties improvements of the UHMWPE/NMWP blends. In Sect. 3.1, the influences of parameters χ and N on the interfacial properties and phase morphologies will be studied first, and then the effects of these parameters on the viscosity and mechanical properties will also be discussed. In Sect. 3.2, we will predict the optimum parameter ranges in which the UHMWPE/NMWP blends not only display two-phase morphologies but also possess thick interfaces.

Effects of parameters χ and N on interfacial properties and phase morphologies

Effect of parameter χ

For the binary UHMWPE/NMWP blends, we fixed molecular chain lengths (N_{UHMWPE}=11600, N_{NMWP}=250) and varied repulsion parameter α from 25.82 to 45.42 [χ from 3.2×10^{-3} to 2.5×10^{-2} because α relates to χ via Eq. 14]. Figure 1a and b respectively show the relation between the parameter χ and the simulated interfacial tensions and density profiles of the UHMWPE/NMWP (50/50) blend. It is found that at fixed chain length, an increase in the repulsive interaction parameter enhances interfacial tension (γ) and decreases the dislike contacts between unlike segments UHMWPE and NMWP. As a result, the interfacial region is narrowed. The interfacial tension in each slab is obtained by dividing the simulation box into 100 slabs parallel to the interface and calculating the pressure tensor in each slab [48]

$$2\gamma = \int_{slab} [P_n(z) - P_t(z)]dz. \quad (17)$$

Table 1 The characteristic variables, molecular weight and the corresponding DPD chain length of UHMWPE

Species	δ (Jcm^3)$^{1/2}$	V_{bead} (cm^3/mol)	σ (Nm$^{-1}\times10^{-5}$)	M_{m}	C_{n}	M_{p}	N_{DPD}
UHMWPE	16.8	32.2	35.7	28.1	7.7	2.5×10^6	11600

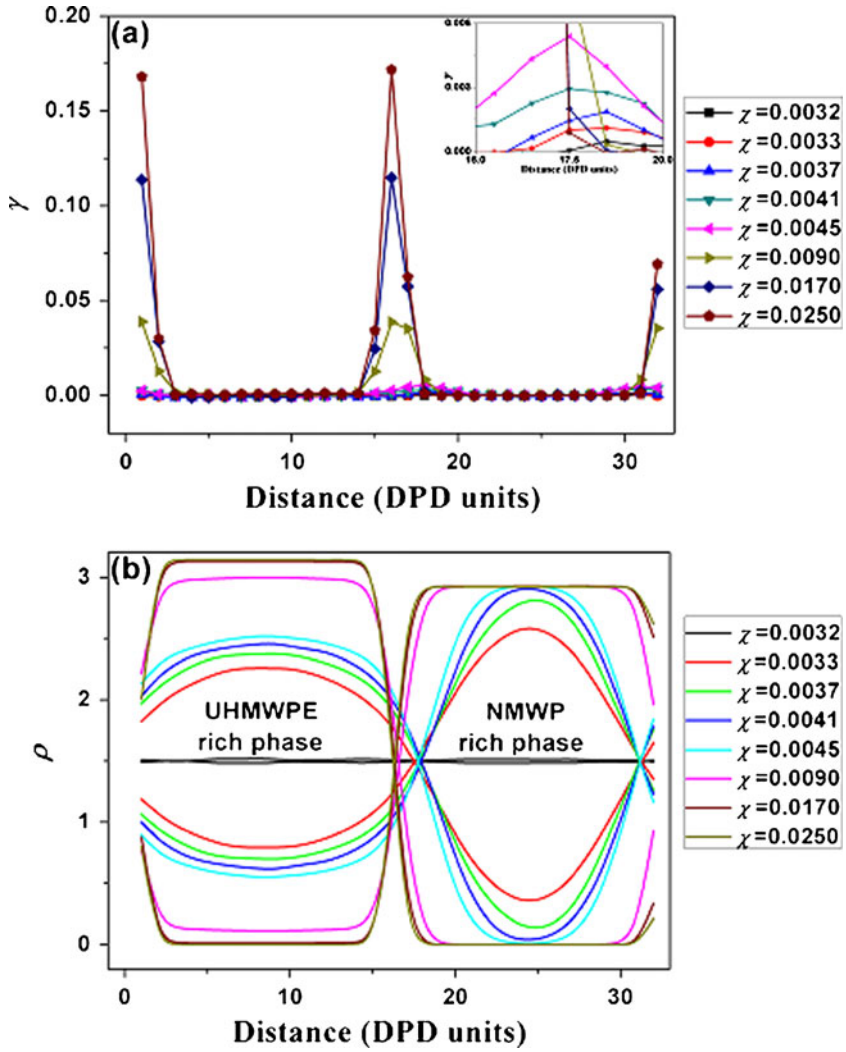

Fig. 1 (**a**) Interfacial tension (γ) and (**b**) Density profiles (ρ) of each component for UHMWPE/NMWP (50/50) blends (N_{UHMWPE}=11600 and N_{NMWP}=250) with different interaction parameter χ

On the left side of this equation, an additional factor 2 arises from the existence of two interfaces in the system due to the periodic boundary conditions. $P_n(z)$ and $P_t(z)$ are the normal and transversal components of the pressure tensors. Their expressions take the forms

$$P_n(z) = \rho(z)k_BT + \frac{1}{A}\left\langle \sum_{i<j} \frac{F_{ij}^z \cdot r_{ij}^z}{r_{ij}^z}\theta\left(\frac{r^z - r_{ij}^z}{r_{ij}^z}\right)\theta\left(\frac{r_j^z - r^z}{r_{ij}^z}\right)\right\rangle \quad (18)$$

$$P_t(z) = \rho(z)k_BT + \frac{1}{2A}\left\langle \sum_{i<j} \frac{F_{ij}^x \cdot r_{ij}^x + F_{ij}^y \cdot r_{ij}^y}{r_{ij}^z}\theta\left(\frac{r^z - r_i^z}{r_{ij}^z}\right)\theta\left(\frac{r_j^z - r^z}{r_{ij}^z}\right)\right\rangle \quad (19)$$

Here $\rho(z)$ denotes the density at z averaged over tangential coordinates x and y, and $\theta(x)$ denotes the Heaviside step function.

In Fig. 1b, each component of the UHMWPE/NMWP (50/50) blend can hardly diffuse into each other's rich phases when χ is larger than 1.7×10^{-2}, leading to thin interfaces, which might bring about significant deterioration in some of the most desirable mechanical properties such as the impact strength [20, 21]. This figure also shows that an increase in the parameter χ favors the formation of two-phase morphologies. When χ is in the range of 9.0×10^{-3}~4.1×10^{-3}, no UHMWPE is located in the NMWP rich phase, which prevents the viscosity of NMWP from increasing. However, there is a significant amount of NMWP in the UHMWPE rich phase, which favors the swelling of UHMWPE powders [16, 17]. When χ is lower than 3.7×10^{-3}, interfacial thickness markedly increases with decreasing χ. For $\chi<3.2\times10^{-3}$, the interfaces disappear and the UHMWPE/NMWP blends finally form homogeneous phase. For the UHMWPE/PP blends ($\chi\approx9\times10^{-3}$), PP preferred to locate in the amorphous or low crystallinity zones of the UHMWPE matrix, and the blend showed two-phase morphologies. However, in the UHMWPE/HDPE blends (χ is about 0), HDPE molecules penetrated into UHMWPE particles during processing because of the good

miscibility of the two polymers, and then homogeneous phase structures appeared. These experimental observations are in agreement with the predictions of the DPD simulations (Fig. 1). As has been stated in the introduction, homogeneous phase morphologies and thin interface are separately unfavorable to the flowability improvement and mechanical properties maintenance of the blends. Therefore, for the UHMWPE/NMWP blends, the value of χ should be in a certain range in which the blends might exhibit favorable processability and mechanical properties.

As is shown in Fig. 2, the end-to-end distance of UHMWPE chain is calculated as a function of χ between the unlike segments in the UHMWPE/NMWP blends using the DPD simulations. It is evident that the end to end distances of UHMWPE chains in the UHMWPE/NMWP blends decrease in the following order: $6.25r_c(\chi=3.2\times10^{-3})>6.11(3.3\times10^{-3})>5.94(3.7\times10^{-3})>5.81(4.1\times10^{-3})>5.76(4.7\times10^{-3})>5.53(9.0\times10^{-3})>5.45(1.7\times10^{-2})>5.40(2.5\times10^{-2})$, which illustrates that the diameters of UHMEPE particles increase with decreasing parameter χ. This indicates that the swelling capability of NMWP on UHMWPE chains increases with decreasing χ, which is in agreement with Fig. 1b.

Effect of molecular chain length and its polydispersity

The effect of molecular chain length of NMWP on the morphologies and interfacial properties of the UHMWPE/NMWP blends (N_{NMWP}=250, 1000, 2000, 3000, 5000, 9000) are also studied by DPD simulation at the fixed N_{UHMWPE} =11600 and χ =2×10^{-3} (Fig. 3). As is shown in Figs. 1 and 3, parameters N and χ have similar effects on interfacial tensions and interfacial thicknesses of the blends. Concretely, interfacial tensions decrease and interfacial thicknesses increase remarkably with N_{NMWP} decreasing from 9000 to 250. When N_{NMWP} is in the range of 2000~9000, interfacial thicknesses change slightly. However, as N_{NMWP} decreases from 2000 to 1000, the interfacial thicknesses and the volume of UHMWPE rich-phase increase significantly, which indicates NMWP molecules can defuse into UHMWPE rich phase. The swelling action of NMWP on UHMWPE is also corroborated by the dramatic increases of end-to-end distances of UHMWPE chains with decreasing N_{NMWP} as is shown in Fig. 4. When N_{NMWP} reaches 250, two-phase structures of the UHMWPE/NMWP blends disappear and homogeneous phase structures occur simultaneously. Therefore, both too small and too large N_{NMWP} might be unfavorable to the viscosity reduction and mechanical improvement, respectively.

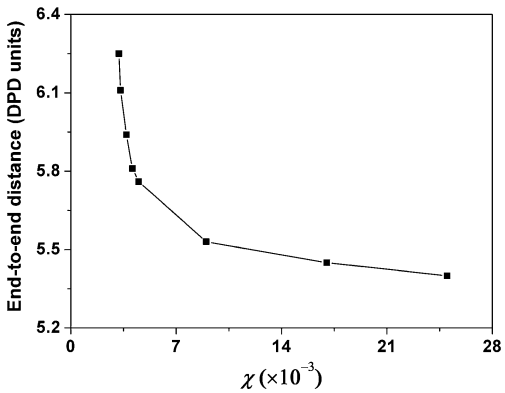

Fig. 2 Simulated dependence of end-to-end distances of UHMWPE chains on χ in the UHMWPE/NMWP (50/50) blends (N_{UHMWPE}= 11600 and N_{NMWP}=250) with different interaction parameter χ

Real polymer samples are polydisperse. It is therefore of great interest to investigate the effect of polydispersity on interfacial properties of the PE/NMWP blends. In this section, the interfaces between polydisperse polymers are analyzed by considering the simplest molten polydisperse system: both PE and NMWP melts include long chain and short chain components. Concretely, long PE (UHMWPE) and short PE (SPE) chains are respectively composed of 11600 and 250 beads while long NMWP (LP) and short NMWP (SP) chains are composed of 1000 and 250 beads.

Figures 5 and 6 show the density profiles of the UHMWPE/SPE/LP/SP blends with different compositions. It can be seen that both UHMWPE and LP prefer to be in their own rich phases. Both SPE and SP, however, are located not only in their own rich phases, but also in their neighbor phases (Fig. 5). Besides, there is a significant accumulation of short chains at the interface, as is indicated in Fig. 6. With increasing concentration of the short chains, this accumulation of the short chains at the interface increases and pushes the long chains further away from the interface. The physical reason of the accumulation can be attributed to the fact that the effect of lowering the interfacial tension can be created by having more short chains at the interface which actually play a surfactant role, as is suggested in Fig. 7.

The above mentioned studies indicate that too small χ and N_{NMWP} may lead to the formation of homogeneous phases of the UHMWPE/NMWP blends. On the contrary, when χ and N_{NMWP} are too large, interfacial tensions will be very large and interfaces will be very thin. Both homogeneous phase structures and thin interfaces are unfavorable to the modification of UHMWPE. In what follows, a phase diagram based on Flory-Huggins theory is adopted to predict the optimal ranges of χ and N_{NMWP}, in which the UHMWPE/NMWP blends can demonstrate both two-phase morphology and thick interface.

Prediction for the optimum ranges of parameters χ and N

Figure 8 displays a phase diagram of the UHMWPE/NMWP blends, plotted in χ vs ϕ_{UHMWPE}. A representative

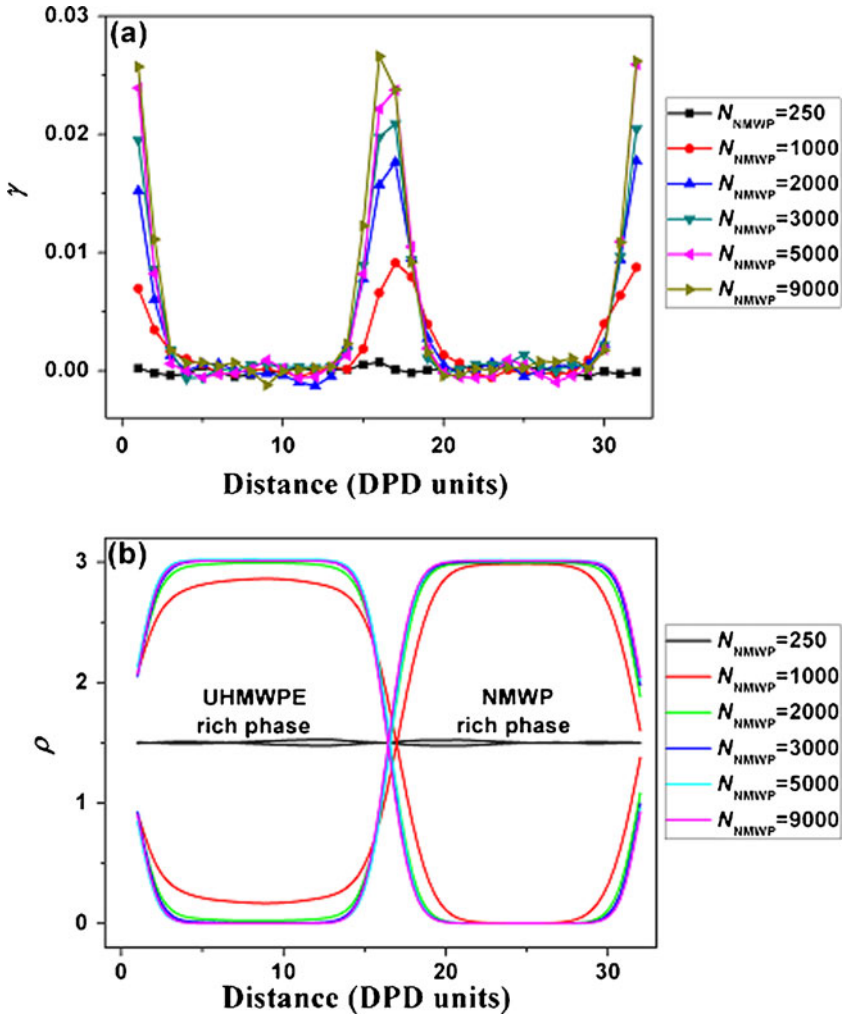

Fig. 3 (**a**) Interfacial tension and (**b**) Density profiles of each component in UHMWPE/NMWP (50/50) blends (N_{UHMWPE}=11600 and χ=0.002) with different N_{NMWP}

phase diagram (N_{NMWP}=250; N_{UHMWPE}=11600) is plotted to discuss the general properties of these blends. To test and verify the accordance between the results of Flory-Huggins theory calculation and DPD simulation on the UHMWPE/NMWP blends, we carry out DPD simulation on these systems whose parameters respectively located in each typical region of the phase diagram such as single phase, two-phase and metastable regions. The simulated density profiles and morphologies are shown in Figs. 1 and 8. For the parameters (ϕ_{UHMWPE}, χ) below binodal curve such as (0.5, 0.0032), the blend possesses a homogeneous phase [Fig. 8a]. On the contrary, when the parameters (ϕ_{UHMWPE}, χ) are above spinodal curve such as (0.5, 0.0045), two-phase structure of the UHMWPE/NMWP blends occur with very thin interface and large interfacial tension (Figs. 1 and 8e). However, for the parameters (ϕ_{UHMWPE}, χ) between binodal and spinodal curves, such as (0.5, 0.0033), (0.5, 0.0037) and (0.5, 0.0041), not only the blends virtually separate into two phases, but also the interface is very thick, as Figs. 1 and 8b–d show. Therefore, the parameters (ϕ_{UHMWPE}, χ) in metastable region are beneficial to both the viscosity reduction and the mechanical properties maintenance of the UHMWPE/NMWP (50/50) blends. Besides, Fig. 8 also suggests that the DPD simulated results are in good agreement with the predictions based on Flory-Huggins theory.

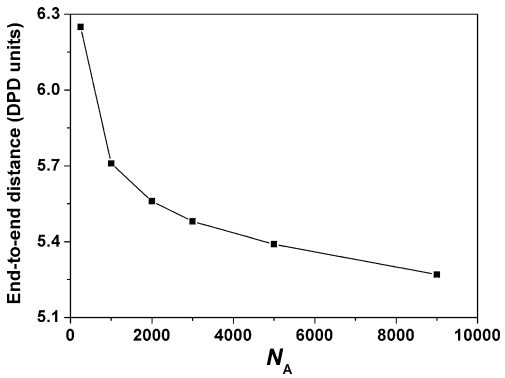

Fig. 4 Simulated dependence of end-to-end distance of UHMWPE on NMWP in UHMWPE/NMWP (50/50) blends (N_{UHMWPE}=11600 and χ=0.002) with different N_{NMWP}

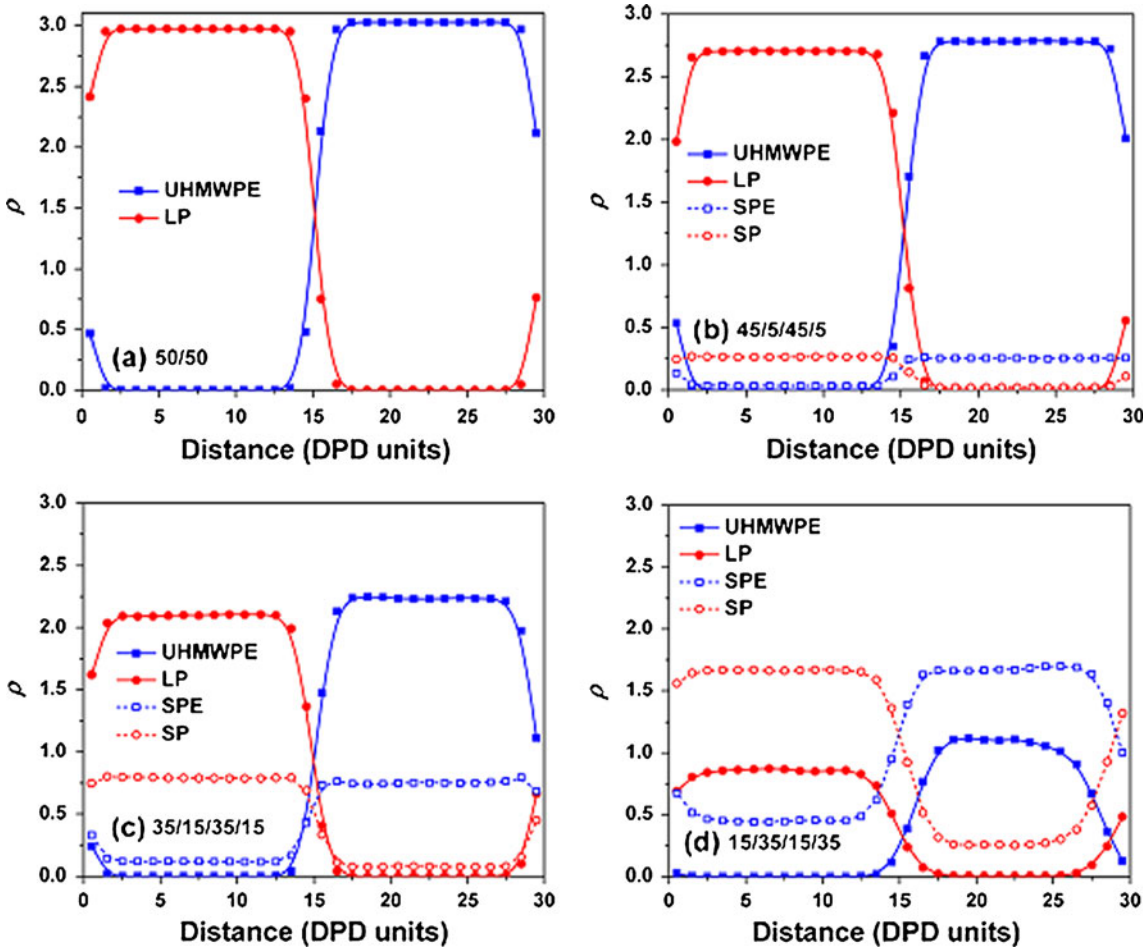

Fig. 5 Density profiles of each component for the blends: (**a**) UHMWPE/LP; (**b**), (**c**), (**d**) UHMWPE/SPE/LP/SP

The effects of N_{NMWP} on the morphologies and interfacial properties of the UHMWPE/NMWP blends with fixed N_{UHMWPE} (11600) are also studied by phase diagram, which is shown in Fig. 9. The results indicate that both binodal and spinodal curves shift downward with increasing N_{NMWP}, which suggests that the increase of N_{NMWP} is favorable to the phase separation of the UHMWPE/NMWP blends. The DPD simulation is also carried out on the UHMWPE/NMWP blends, in which χ, ϕ_{UHMWPE}, N_{UHMWPE} are taken as 0.002, 0.5, 11600, and N_{NMWP} is in the range of 250–1000 [Fig. 9a–e]. This phase diagram

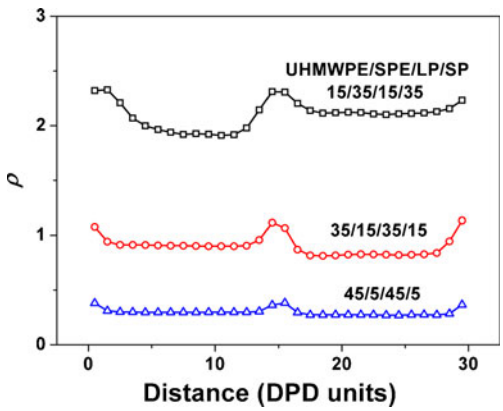

Fig. 6 The sum of the densities of SPE and SP in the blends UHMWPE/SPE/LP/SP

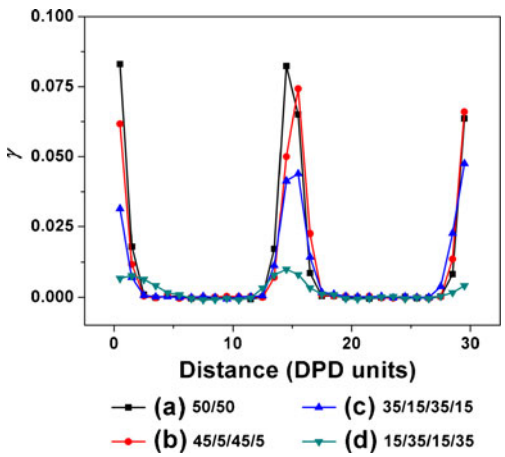

Fig. 7 Interfacial tension for: (**a**) UHMWPE/ LP; (**b**), (**c**), (**d**) UHMWPE/SPE/LP/SP

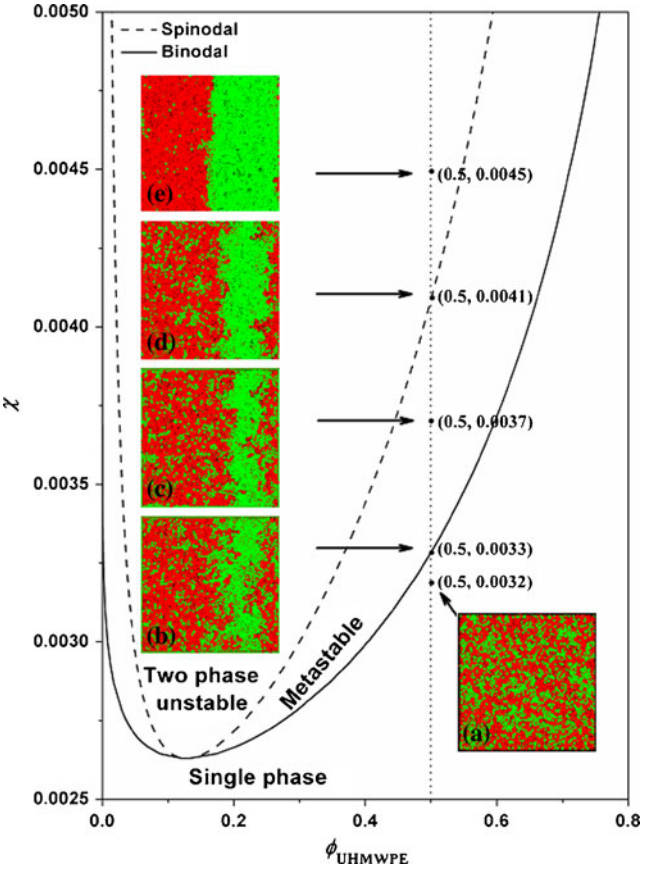

Fig. 8 Simulated phase diagram for the UHMWPE/NMWP (50/50) blend (N_{UHMWPE}=11600, N_{NMWP}=250) plotted in χ vs ϕ_{UHMWPE}. Morphologies of the blends with various χ (from 0.0032 to 0.0045) are also simulated by DPD. Green and red beads represent NMWP and UHMWPE, respectively

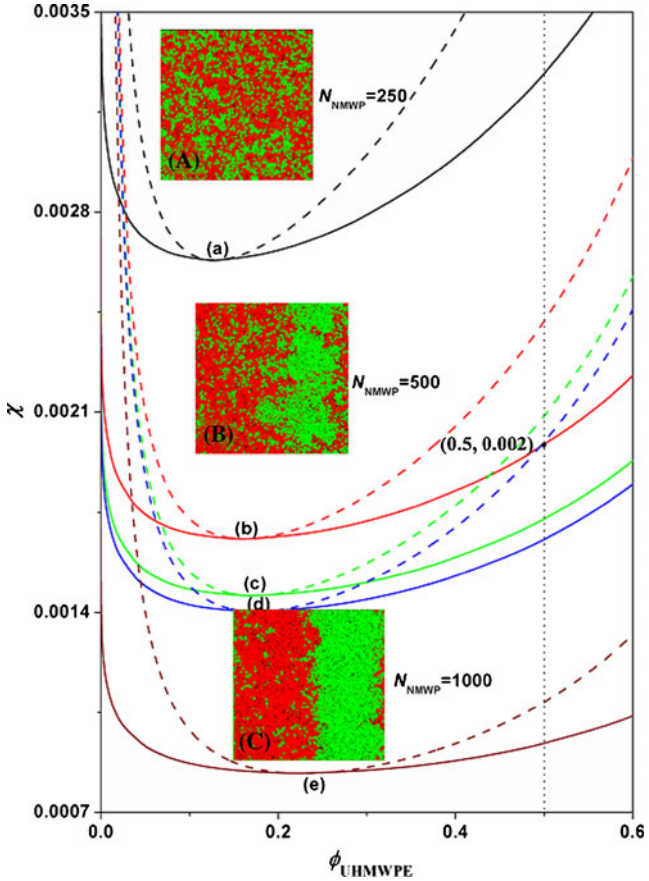

Fig. 9 Phase diagrams for the UHMWPE/NMWP (50/50) blend with fixed N_{UHMWPE}=11600 and various N_{NMWP}: (**a**) N_{NMWP}=250; (**b**) 429; (**c**) 500; (**d**) 524; (**e**) 1000. Morphologies of the blends with fixed χ (0.002), N_{UHMWPE} (11600) and various N_{NMWP} [(**A**), (**B**), (**C**) corresponding to (**a**), (**c**) and (**e**)] are also simulated by DPD. Green and red beads represent NMWP and UHMWPE, respectively

indicates that the effects of N_{NMWP} are three fold. Firstly, when N_{NMWP}<429, the parameter [ϕ_{UHMWPE} (0.5), χ (0.002)] is located below binodal curve, and each component homodisperses in the UHMWPE/NMWP blends, as is shown in Fig. 10a. Secondly, when N_{NMWP}>524, the parameter (0.5, 0.002) is located above spinodal curve. In this case, two-phase morphologies occur and the interface is very thin [Fig. 9c]. Thirdly, when N_{NMWP} is in the range of 429~524, the parameter (0.5, 0.002) is located in the metastable region of the UHMWPE/NMWP blends. The blends not only show two-phase morphologies but also thick interface between two components. Hence, N_{NMWP} in the UHMWPE/NMWP blends with parameters (ϕ_{UHMWPE}, χ) in the metastable region is also favorable to both the viscosity reduction and mechanical properties maintenance.

The influence of N_{NMWP} and χ on interfacial properties and morphologies of the UHMWPE/NMWP (50/50) blends have been studied separately in the above mentioned DPD simulations and theoretical predictions. In this part, Flory-Huggins theory is also performed on the predictions of the simultaneous influences of both parameters χ and N_{NMWP} on the blends with different N_{UHMWPE} and ϕ_{UHMWPE} as shown in Fig. 10, in which A, B and C represent two-phase, metastable and homogeneous phase regions, respectively. The UHMWPE/NMWP blends with parameters (χ, N_{NMWP}) in B region will show two-phase morphologies and thick interfaces, so B region is advisable for the modification of UHMWPE. If NMWP, for example, is polyisobutene, the available volume fraction and molecular weight should be about 0.05 and 9.0×10^4 g mol^{-1}, which are calculated by Flory-Huggins theory. If NMWP is polypropylene, for another example, its volume fractions and molecular weight should be about 0.12 and 7.2×10^4 g mol^{-1}. Some of the commonly used blends for improving the processing properties of UHMWPE can satisfy the requirements discovered in this work [17, 49, 50]. For example, Liu's study indicated that adding 10 wt % PP into UHMWPE not only could decrease the apparent melt viscosity of UHMWPE significantly, but also could improve the Yield strength, strength at break and Young's modulus in different degrees. The realistic molec-

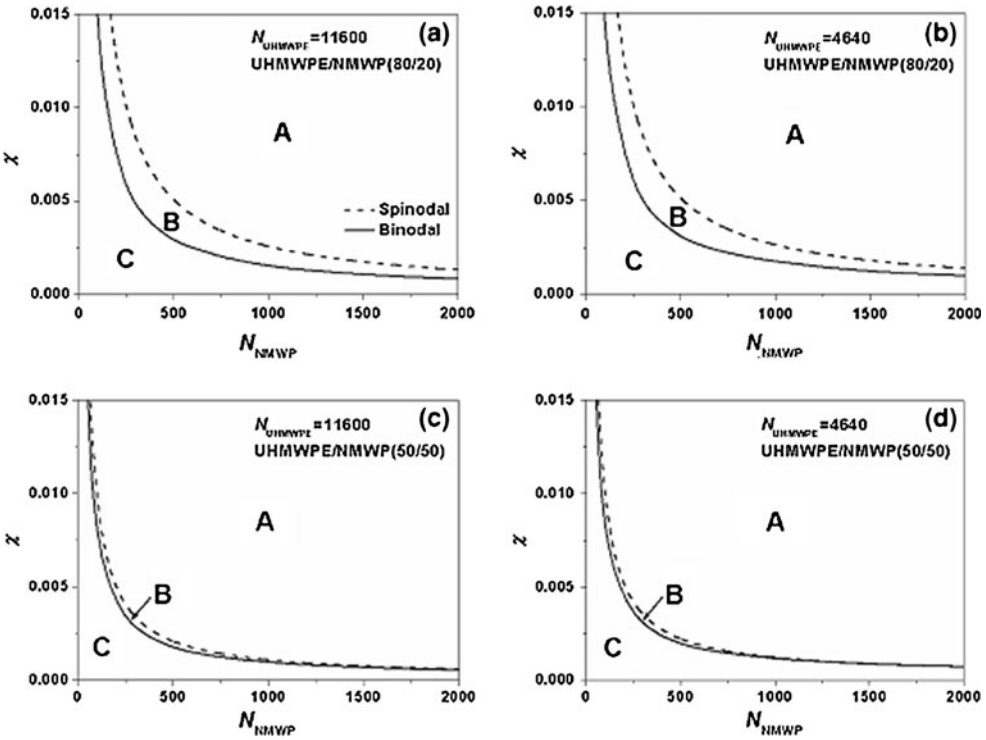

Fig. 10 Phase diagrams for the UHMWPE/NMWP blend with different N_{UHMWPE} and composition. **A**, **B** and **C** correspond to two-phase, metastable and homogeneous phase regions, respectively

ular weight of PP used in Liu's study is 1.1×10^5 g mol^{-1}. The corresponding chain length is 376 (calculated by Eq. 16). For the blend UHMWPE/PP (90/10) in Liu's studies, the corresponding parameters including the volume fraction and chain length of PP fall in the metastable region of its phase diagram. Hence, this experimental study is consistent with the findings of the present work. The comparisons of the B regions in Fig. 10a and b (or c and d) suggest that the area of B region change slightly when N_{UHMWPE} is in the range of 4640~11600. However, by comparing Fig. 10a and c (or b and d), it is easy to find that the area of B region increases significantly with increasing ϕ_{UHMWPE} from 0.5 to 0.8, which indicates that there is a wider range of optional N_{NMWP} in modification of UHMWPE at higher ϕ_{UHMWPE}.

Conclusions

In this work, we have investigated the effects of interaction parameter and molecular chain length on the morphologies and interfacial properties of the UHMWPE/NMWP blends by DPD simulation and theoretical predictions.

Interaction parameter χ and molecular chain length N_{NMWP} have similar effects on interfacial tensions and interfacial thicknesses of the blends. Increase of parameters χ and N_{NMWP} enhances the interfacial tension and decreases the dislike contacts between unlike segments UHMWPE and NMWP. As a result, the interfacial region is narrowed. For polydisperse UHMWPE blends, there is a significant accumulation of short chains at the interface. The physical reason of the accumulation can be attributed to the fact that the effect of lowering the interfacial tension can be created by having more short chains at the interface, which actually play a surfactant role.

Both DPD simulation and theoretical predictions indicate that too small χ and N_{NMWP} may lead to the formation of homogeneous phases of the UHMWPE/NMWP blends. When χ and N_{NMWP} are too large, however, interfacial tension will be very large and interfacial thickness will be very thin. Only when the parameters χ and N_{NMWP} are located in metastable region can the blends show two-phase morphologies and thick interfaces. Therefore, metastable region is advisable for both the viscosity reduction and mechanical improvement of the UHMWPE/NMWP blends.

Acknowledgments This work was supported by the National Natural Science Foundation of China (51003067), and Fundamental Research Funds for the Central Universities.

References

1. Oral E, Beckos CG, Muratoglu OK (2008) Free radical elimination in irradiated UHMWPE through crystal mobility in phase transition to the hexagonal phase. Polymer 49:4733–4739
2. Prever EB, Crova M, Costa L, Dallera A, Camino G, Gallinaro P (1996) Unacceptable biodegradation of polyethylene in vivo. Biomaterials 17:873–878
3. Furmanski J, Pruitt LA (2007) Peak stress intensity dictates fatigue crack propagation in UHMWPE. Polymer 48:3512–3519

4. Gai JG, Li HL, Schrauwen C, Hu GH (2009) Dissipative particle dynamics study on the phase morphologies of the ultrahigh molecular weight polyethylene/ polypropylene/ poly(ethylene glycol) blends. Polymer 50:336–346
5. Zhang QH, Lippits DR, Rastogi S (2006) Dispersion and Rheological Aspects of SWNTs in Ultrahigh Molecular Weight Polyethylene. Macromolecules 39:658–666
6. Gai JG, Li HL (2007) Ultrahigh molecular weight polyethylene/ polypropylene/ organo -montmorillonite nanocomposites: Phase morphology, rheological, and mechanical properties. J Appl Polym Sci 106:3023–3032
7. Wen JP, Yin P, Zhen MH (2008) Friction and wear properties of UHMWPE/nano-MMT composites under oilfield sewage condition. Mater Lett 62:4161–4163
8. Gai JG, Li HL (2007) Influence of organophilic montmorillonite and polypropylene on the rheological behaviors and mechanical properties of ultrahigh molecular weight polyethylene. J Appl Polym Sci 105:1200–1209
9. Bin Y, Lin M, Alachi R (2001) Ultra-drawing of low molecular weight polyethylene — ultra-high molecular weight polyethylene blend films prepared by gelation/ crystallization from semi-dilute solutions. Polymer 42:8125–8135
10. Mastuo M, Manley R (1982) Ultradrawing at room temperature of high molecular weight polyethylene. Macromolecules 15:985–987
11. Zuo JD, Zhu YM, Liu SM, Jiang ZJ, Zhao JQ (2007) Preparation of HDPE/UHMWPE/MMWPE blends by two-step processing way and properties of blown films. Polym Bull 58:711–722
12. Vadhar P, Kyu T (1987) Effects of mixing on morphology, rheology, and mechanical properties of blends of ultra-high molecular weight polyethylene with linear low-density polyethylene. Polym Eng Sci 27:202–210
13. Lee EM, Oh YS, Ha HS, Kim BK (2009) Rheological properties of UHMWPE/iPP blends. Polym Adv Technol 20:1121–1126
14. Xie MJ, Li HL (2007) Viscosity reduction and disentanglement in ultrahigh molecular weight polyethylene melt: Effect of blending with polypropylene and poly(ethylene glycol). Eur Polym J 43:3480–3487
15. Takeshi S, Kyouji M, kunie H (1989) EP 0315481A2
16. Liu GD, Chen YZ, Li HL (2004) Study on processing of ultrahigh molecular weight polyethylene/polypropylene blends. J Appl Polym Sci 94:977–985
17. Liu GD, Chen YZ, Li HL (2004) Study on processing of ultrahigh molecular weight polyethylene/polypropylene blends: Capillary flow properties and microstructure. J Appl Polym Sci 92:3894–3900
18. Li XM, Zhou W, Jiang T (2008) Preparation of UHMWPE/PLA blends. China Synthetic Resin and Plastics 25:11–15
19. Sawatari C, Matsuo M (1989) Morphological and mechanical properties of ultrahigh-molecular-weight polyethylene/low-molecular-weight polyethylene blend films produced by gelation/ crystallization from solutions. Polymer 30:1603–1614
20. Wu S (1982) Polymer Interfaces and Adhesion. Marcel Dekker, New York
21. Koberstein JT (1987) In Encyclopedia of Polymer Science and Engineering. Wiley, New York
22. Liang BR, White JL, Spruiell JE, Goswami BC (1983) Polypropylene/nylon 6 blends: Phase distribution morphology, rheological measurements, and structure development in melt spinning. J Appl Polym Sci 28:2011–2032
23. Min K, White JL, Fellers JF (1984) High density polyethylene/ polystyrene blends: Phase distribution morphology, rheological measurements, extrusion, and melt spinning behavior. J Appl Polym Sci 29:2117–2142
24. Scheetz HA, Gilles RC (1981) U.S. Pat. 4,281,070
25. Liu GD, Li HL (2003) Extrusion of ultrahigh molecular weight polyethylene under ultrasonic vibration field. J Appl Polym Sci 89:2628–2632
26. Lee WJ, Ju SP, Wang YC (2007) Modeling of polyethylene and poly (L-lactide) polymer blends and diblock copolymer: Chain length and volume fraction effects on structural arrangement. J Chem Phys 127:064902–064913
27. Yang H, Li ZS, Lu ZY, Sun CC (2005) Computer simulation studies of the miscibility of poly(3-hydroxybutyrate)-based blends. Eur Polym J 41:2956–2962
28. Anastasiadis SH, Ganzarz I, Koberstein JT (1988) Interfacial tension of immiscible polymer blends: temperature and molecular weight dependence. Macromolecules 21:2980–2987
29. Groot RD, Madden TJ, Tildesley DJ (1999) On the role of hydrodynamic interactions in block copolymer microphase separation. J Chem Phys 110:9739–9750
30. Shillcock JC, Lipowsky R (2002) Equilibrium structure and lateral stress distribution of amphiphilic bilayers from dissipative particle dynamics simulations. J Chem Phys 117:5048–5062
31. Tsige M, Grest GS (2004) Molecular dynamics simulation of solvent–polymer interdiffusion: Fickian diffusion. J Chem Phys 120:2989–2996
32. Groot RD, Rabone KL (2001) Mesoscopic Simulation of Cell Membrane Damage, Morphology Change and Rupture by Nonionic Surfactants. Biophys J 81:725–836
33. Wijmans CM, Smit B, Groot RD (2001) Phase behavior of monomeric mixtures and polymer solutions with soft interaction potentials. J Chem Phys 114:7644–7655
34. Flory PJ (1942) Principles of Polymer Chemistry. Cornell University, New York
35. Huggins ML (1942) Some Properties of Solutions of Long-Chain Compounds. J Phys Chem 46:151–158
36. Qian CB, Mumby SJ, Eichinger BE (1991) Phase Diagrams of Binary Polymer Solutions and Blends. Macromolecules 24:1655–1661
37. Rubinstein M, Colby RH (2003) Polymer Physics. Oxford University Press, Wellington
38. Groot RD, Warren PB (1997) Dissipative particle dynamics: Bridging the gap between atomistic and mesoscopic simulation. J Chem Phys 107:4423–4436
39. Español P, Warren PB (1995) Statistical mechanics of dissipative particle dynamics. Europhys Lett 30:191–196
40. Groot RD, Madden TJ (1998) Dynamic simulation of diblock copolymer microphase separation. J Chem Phys 108:8713–8725
41. Case FH, Honeycutt JD (1994) Will my polymer mix? Methods for studying polymer miscibility. Trends Polym Sci 2:256–258
42. Rogers D, Hopfinger AJ (1994) Application of Genetic Function Approximation to Quantitative Structure-Activity Relationships and Quantitative Structure-Property Relationships. J Chem Inf Comput Sci 34:854–866
43. Liu DH, Zhong CL (2006) Cooperative Self-Assembly of Nanoparticle Mixtures in Lamellar Diblock Copolymers: A Dissipative Particle Dynamics Study. Macromol Rapid Commun 27:458–462
44. Groot RD (2003) Electrostatic interactions in dissipative particle dynamics—simulation of polyelectrolytes and anionic surfactants. J Chem Phys 118:11265–11278
45. Özen AS, Sen U, Atilgan C (2006) Complete mapping of the morphologies of some linear and graft fluorinated co-oligomers in an aprotic solvent by dissipative particle dynamics. J Chem Phys 124:064905–064914
46. Liu DH, Zhong CL (2008) Multicompartment micelles formed from star-dendritic triblock copolymers in selective solvents: A dissipative particle dynamics study. Polymer 49:1407–1413

47. Jawalkar SS, Aminabhavi TM (2006) Molecular modeling simulations and thermodynamic approaches to investigate compatibility/incompatibility of poly(l-lactide) and poly(vinyl alcohol) blends. Polymer 47:8061–8071
48. Varnik F, Baschnagel J, Binder K (2002) Molecular dynamics results on the pressure tensor of polymer films. J Chem Phys 113:4444–4454
49. Zhang T, Zou XX, Zhang SJ, Yang W, Yang MB (2009) Effect of entropy penalty on selective distribution of aluminum borate whiskers in isotactic polypropylene (iPP)/syndiotactic polypropylene (sPP) blends. Polymer 50:3047–3054
50. Liu GD, Xiang M, Li HL (2004) A study on sliding wear of ultrahigh molecular weight polyethylene/polypropylene blends. Polym Eng Sci 44:197–208